

Article

Improved Reliability and Mechanical Performance of Sn58Bi Solder Alloys

Guang Ren * and Maurice N. Collins *

Stokes Laboratories, Bernal Institute, University of Limerick, Ireland

* Correspondence: maurice.collins@ul.ie (M.C.), guang.ren@ul.ie (G.R.)

Abstract: Microstructural and mechanical properties of the eutectic Sn58Bi and micro-alloyed Sn57.6Bi0.4Ag solder alloys were compared. With the addition of Ag micro-alloy, the tensile strength was improved and this is attributed to a combination of microstructure refinement and an Ag₃Sn precipitation hardening mechanism. However, ductility is slightly deteriorated due to the brittle nature of the Ag₃Sn intermetallic compounds (IMCs). Additionally, a board level reliability study of Ag micro-alloyed Sn58Bi solder joints produced utilising a surface-mount technology (SMT) process, were assessed under accelerated temperature cycling (ATC) conditions. Results reveal that micro-alloyed Sn57.6Bi0.4Ag has a higher characteristic lifetime with a narrower failure distribution. This enhanced reliability corresponds with improved bulk mechanical properties. It is postulated that Ag₃Sn IMCs are located at the Sn-Bi phase boundaries and suppress the solder microstructure from coarsening during the temperature cycling, hereby extending the time to failure.

Keywords: Sn58Bi, Ag, Micro-alloy, Mechanical, Reliability

1. Introduction

The implementation of legislation entitled “Restriction on the use of certain Hazardous Substances (RoHS)” in the European Union in July 2006 marked the beginning of the phasing out of conventional Sn-37Pb eutectic solder in the electronic industry. RoHS has been since adopted in countries and regions with dense electronics manufacturing: Korea, Japan, China and a range of US states [1]. In response, most major electronics manufacturers have stepped up their search for alternatives to Pb-containing (Sn-37Pb) solders, i.e., Pb-free solders. Sn-Ag, Sn-Cu and Sn-Ag-Cu (SAC) Pb-free eutectic or near eutectic systems have emerged as the front runners in the replacement of Sn-37Pb solder [2]. Among them, near-eutectic SAC alloys have established themselves as the interconnect materials of choice for the electronic packaging industry [3-7]. Various SAC alloy systems have been proposed by Japanese (SAC305, short for Sn-3.0Ag-0.5Cu), EU (SAC387, short for Sn-3.8Ag-0.7Cu) and US (SAC396, short for Sn-3.9Ag-0.6Cu) consortiums [8], with the SAC305 alloy widely used by the industry as the most promising candidate for reliable Pb-free solder due to its reliability under thermal cycling [9, 10].

Comparing conventional Sn-37Pb eutectic solder (183 °C), the higher melting temperature of SAC305 (217 – 221 °C) limits its application when facing miniaturisation challenges associated with emerging ultra-mobile computing, wearable devices, and the Internet of Things (IoT) markets [11]. Therefore, further studies have been carried out globally by industrial as well as academic consortiums on new Pb-free alternatives [12-14]. Sn58Bi solder is gaining considerable attention because of its low melting temperature of 138 °C [15, 16], with other advantages of Sn-Bi-based solder associated with good solderability, superior mechanical properties, good joint strength, excellent creep resistance, low coefficient of thermal expansion (CTE, $1.5 \times 10^{-5}/^{\circ}\text{C}$), and low cost [17].

A range of different nano particles have been added to Sn58Bi-based solder to investigate their effects. For example, Al₂O₃ nanoparticles were reported to strengthen the thermal properties,

corrosion resistance and creep performance [18]. Graphene nanosheets were found to refine the microstructure, enhance the wettability, corrosion resistance, tensile strength, ductility, hardness and creep performance [19]. SiC nanoparticles were found to increase the shear strength of solder bumps on Si wafer, attributed to grain refinement and dispersion hardening [20]. In addition, nano-structured cage-type polyhedral oligomeric silsesquioxane (POSS) were introduced to inhibit oxidation processes under high humidity and temperature, therefore mitigating Sn whisker growth in Sn58Bi, which is expected to benefit its reliability [21].

Micro-alloying, by addition of a trace amount of third element, is also believed to enhance the performance of Sn58Bi-based solder. Ni was found to refine the initial microstructure and enhance the tensile strength [22]. Zn was found to refine the microstructure as well as suppress the microstructure coarsening during aging, resulting in improved elongation and ultimate tensile strength (UTS) both before and after thermal aging [23]. Ti was also found to refine the microstructure, improve both UTS and yield strength (YS), even after aging [24]. Sb was reported to form SnSb IMCs that precipitated finely from the solid Sn solution near the grain boundaries with Bi, and they suppressed the coarsening of the eutectic structure [25]. Rare earth (RE) elements such as Ce and La were found to greatly improve the wettability and shear strength of solder joints, as well as decrease the intermetallic layer (IML) thickening on Cu substrate [26]. Ag was reported to increase the alloy ductility, attributed to a substantial refinement of solidified microstructure [27]. More details regarding effects of micro-alloying on Sn-Bi solder can be found in a comprehensive review produced by the authors [13].

Sun et. al. studied the effects of both Ag micro-alloy and Ag nano particles on Sn58Bi-based solder on electroless nickel immersion gold (ENIG) substrate, revealing that micro-alloyed Sn57.6Bi0.4Ag solder joints had better mechanical properties than nano particle reinforced Sn58Bi + 0.4Ag solder joints after long-time aging, due to serious degeneration of Ag nanoparticle reinforcement [28]. Therefore, micro-alloyed Sn57.6Bi0.4Ag solder is selected in this study to conduct a joint scale reliability study.

The effect of micro-alloying Ag on Sn58Bi-based solder has been studied by different groups [25-29]. Although well studied, a board level joint scale reliability study of Ag micro-alloyed Sn58Bi solder joints produced with SMT has not been reported and this is essential to assess its viability as a SnPb replacement. The combination of thermal fatigue and solder joint creep is considered to be a predominant failure mechanism of electronic assemblies, and it is of particular interest to end users requiring high reliability [30]. ATC is a widely used reliability evaluation technique that simultaneously produces static and strain-induced microstructural evolution in solders as a result of thermal expansion mismatch, thereby accelerating fatigue and creep damage mechanisms [10, 12, 31-36]. In this article, board level reliability of Sn58Bi-based solders is fully investigated using ATC. The influence of micro-alloying Ag on the mechanical performance and reliability of Sn58Bi is fully elucidated utilising Sn37Pb as a control.

2. Materials and Methods

Alloys consisting of Sn-58Bi and Sn-57.6Bi-0.4Ag were provided by Henkel (Hemel Hempstead, UK). The alloy was melted in a stainless steel crucible at 450 °C and chill cast in a custom designed stainless steel mould at room temperature, to form a thick dog-bone shaped ingot. The ingot was then sliced into tensile specimens of 2 mm thickness, as shown in Figure 1. The as-cast solder alloys were cross-sectioned, metallographically polished, and examined using scanning electron microscope (SEM, Hitachi TM1000).

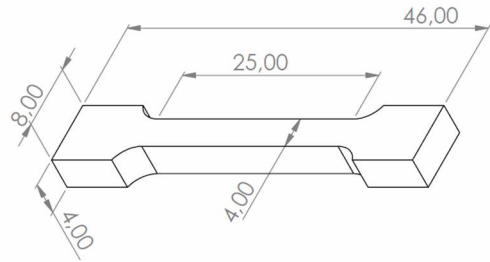


Figure 1. Schematic diagram of the specimen for tensile test (unit: mm)

Tensile tests were performed at room temperature at the strain rate of 0.75 mm/min ($5 \times 10^{-4} \text{ s}^{-1}$) on a tensile test instrument (Tinius Olsen H25KS). A Zwick ZHV30 Vickers hardness tester was used to determine the hardness of as-cast solder alloys. For each composition, 5 tests are carried out to achieve a statistical result. A phase identification of the various solder were carried out using an X-ray diffractometer (XRD, Phillips X'pert) operated at 40 kV, and the Cu-K α radiation was used at diffraction angles (2θ) from 10° to 90° with a scanning speed of $1.2^\circ/\text{min}$.

In addition, two solder pastes, Sn-58Bi and Sn-57.6Bi-0.4Ag were produced utilising a rosin-based flux. Commercial Sn-37Pb solder paste was used in this study as a control. As shown in Figure 2, dummy components consisting 16 of 1206 chip resistors were soldered with these pastes on a FR4 PCB with a Cu OSP surface finish,. The PCB is 1.55mm thick and consisted of 2 layers. A standard right angle 37 pin D-type male connector was used to connect the PCB to an external data logger.

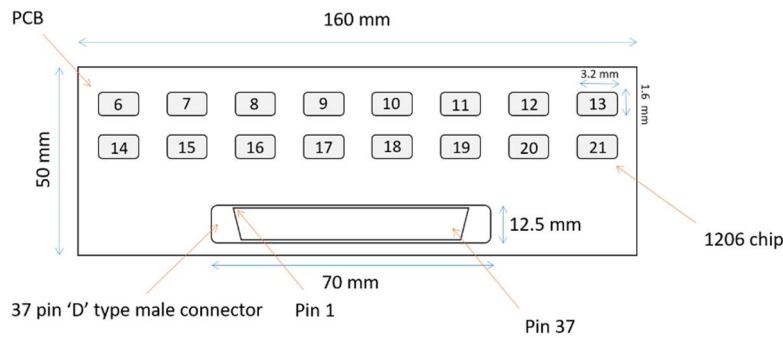


Figure 2. PCB test board, including 16 of 1206 chip resistors and type-D external connector

A Weiss WT -180/40/5 thermal cycling chamber was used to generate thermal cycling for all test vehicles. A 0 – 100°C cycle was imposed, which had the ramp rate 6.7 °C/min on heating and 4 °C/min on cooling. The dwell times were 10 min at both the high and low extremes of the cycle. During ATC, the solder joints were monitored continuously with an Anatech (model 128/256 STD) event detector set at a resistance limit of 1000 Ω . Data were recorded and stored using the WinDatalog software. In accordance with the IPC-9701A industry test guideline, a spike of 1000 Ω for 0.2 ms followed by 9 additional events within 10% of the cycles to the initial event is marked as a failure [37].

3. Results

3.1 Microstructural

The microstructure of as-solidified Sn58Bi and Sn57.6Bi-0.4Ag solder alloys are shown in Figure 3 and Figure 4. The microstructure of Sn58Bi alloy is made up of two phases, Sn phase (black area) and Bi phase (white area). This has been identified in XRD patterns shown in Figure 5. Sn57.6Bi-0.4Ag shows a slightly more refined microstructure than Sn58Bi.

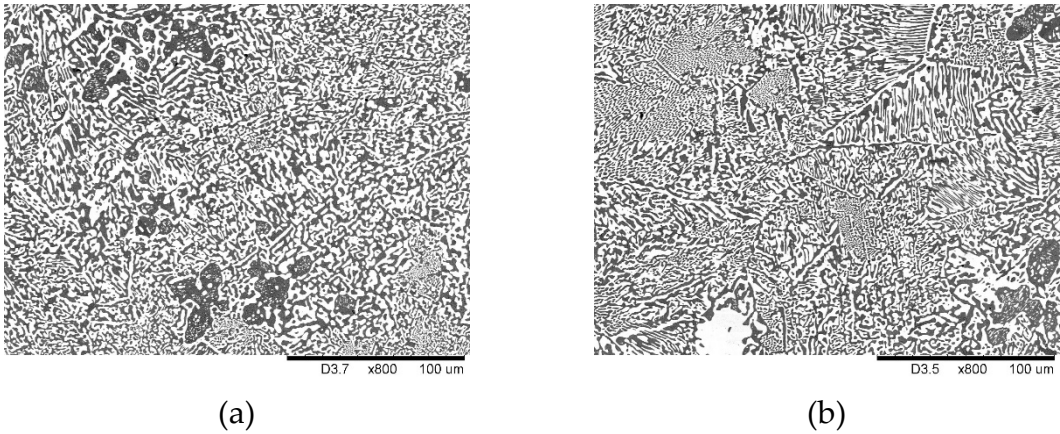


Figure 3. Microstructure at lower magnification (×800): (a) Sn58Bi and (b) Sn57.6Bi0.4Ag

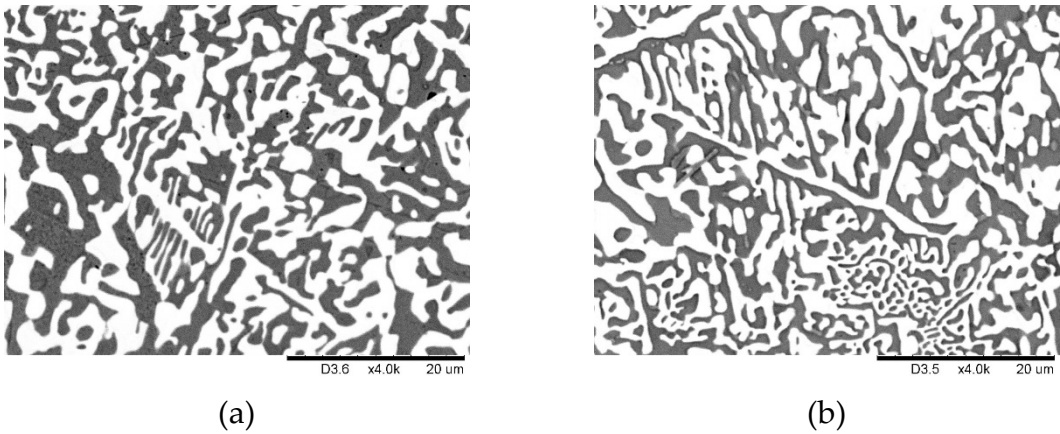


Figure 4. Microstructure at higher magnification (×4000): (a) Sn58Bi and (b) Sn57.6Bi0.4Ag

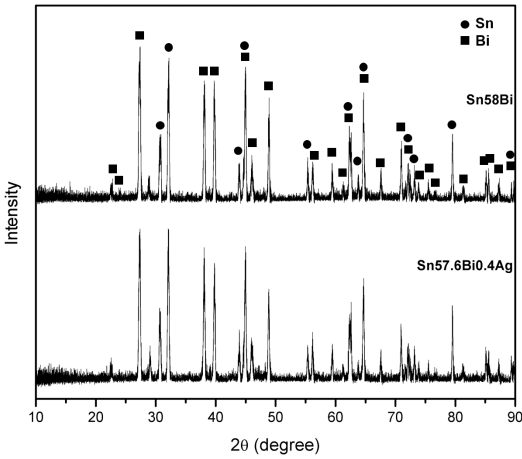


Figure 5. XRD patterns of Sn58Bi and Sn57.6Bi0.4Ag

In the microstructure of Sn57.6Bi0.4Ag, an extra rod-like phase can be observed, as shown in Figure 6. According to the phase diagram of Sn-Bi-Ag as shown in Figure 7, this phase is confirmed to be Ag₃Sn IMCs precipitated from from Sn matrix. However, Ag₃Sn phase has not been detected in XRD, presumably due to its limited content.

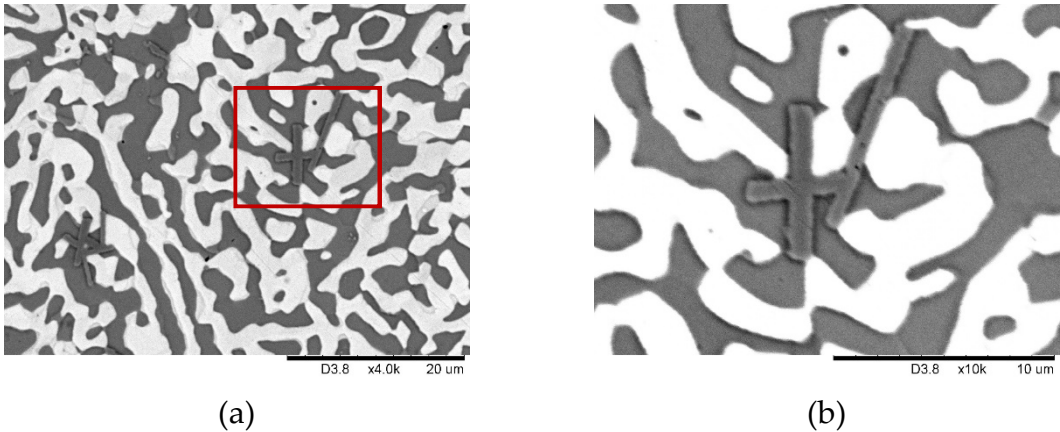


Figure 6. Rod-like phase discovered in Sn57.6Bi0.4Ag solder alloy: (a) ×4000 magnification and (b) ×10000 magnification

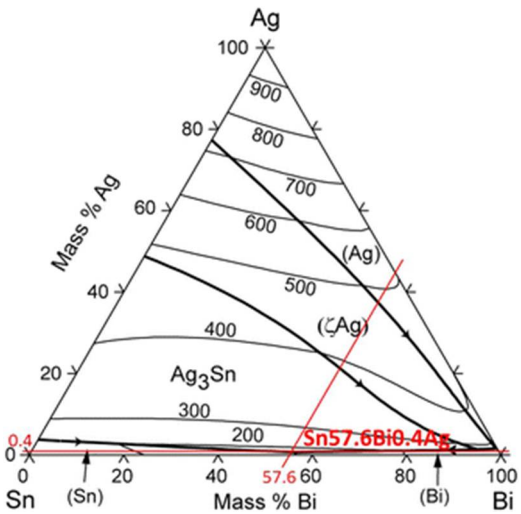


Figure 7. The phase diagram of Sn-Bi-Ag alloy [28]

3.2 Mechanical

Figure 8 shows the typical tensile stress-strain curves of Sn58Bi-based solder alloys. UTS, YS (represented by 0.2% proof stress), elongation, Young’s modulus and micro-hardness of each alloy are listed in Table 1 as well as presented in Figure 9. It can be clearly observed that UTS, YS and Young’s modulus of Sn58Bi-based solder alloy are all slightly increased by micro-alloying 0.4 wt.% Ag. UTS of Sn57.6Bi0.4Ag alloy is 58.7 MPa, which is 6.7% higher than that of Sn-37Pb eutectic alloy (55 MPa) [39] and 2.6% higher than that of Sn58Bi (57.2 MPa). It is worth noting that the YS of Sn58Bi solder alloy is improved by 1.8% with addition of 0.4 wt.% Ag, to 46 MPa. Also, the Young’s modulus is raised by 14.7% as compared with Sn58Bi. While the tensile strength has been increased, the Ag micro-alloy has nelegible effect on micro-hardness of Sn58Bi. The elongation, however, is decreased by 10.6%, with Ag addition, compared with that of original Sn58Bi.

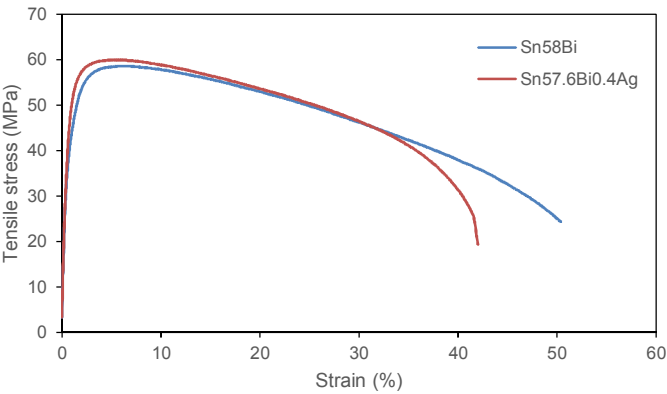


Figure 8. Tensile curves of Sn58Bi and Sn57.6Bi0.4Ag

Table 1. Result of mechanical properties

Alloy	UTS (MPa)	YS (MPa)	Elongation (%)	Young's modulus (GPa)	Micro-hardness (HV)
Sn58Bi	57.2	45.2	54.6	5.0	19.9
Sn57.6Bi0.4Ag	58.7	46.0	48.9	5.7	19.8

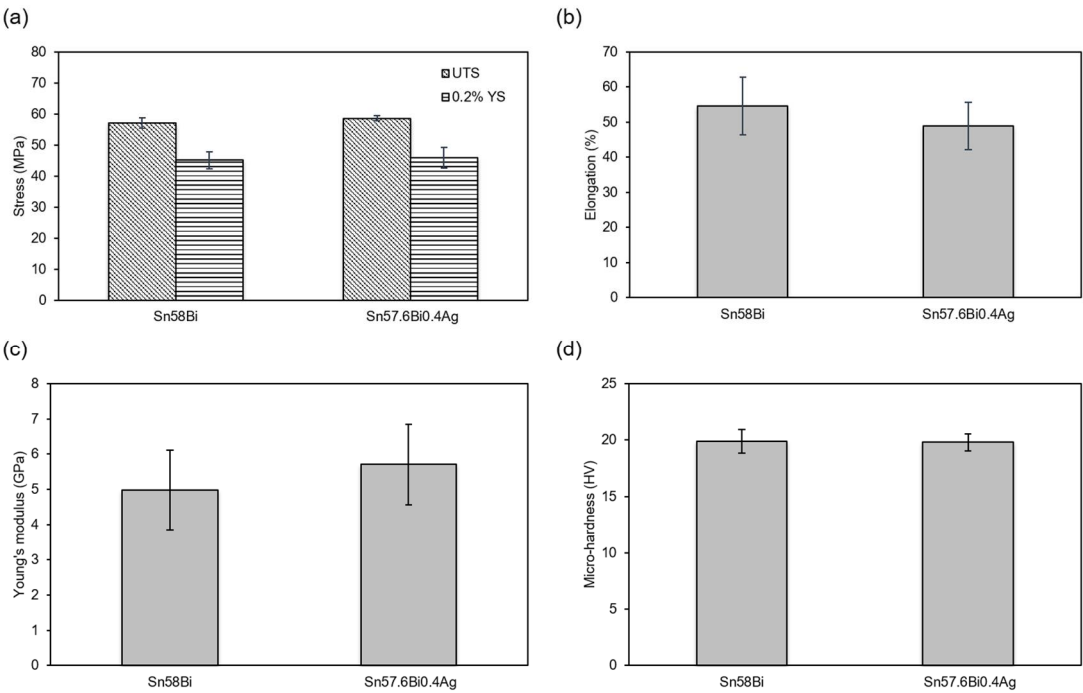


Figure 9. The comparison of mechanical properties: (a) ultimate tensile strength and yield strength, (b) elongation, (c) Young's modulus and (d) micro-hardness, for Sn58Bi and Sn57.6Bi0.4Ag solder alloys.

3.3 Reliability

Reliability data is fit to a two-parameter Weibull distribution:

$$F(t) = 1 - \exp[-(t/\eta)^\beta], \tag{1}$$

where $F(t)$ is the unreliability rate, t is the time (number of cycles) η is the scale parameter (or characteristic life), β is the shape parameter (or slope).

The two-parameter Weibull distribution is shown in Figure 10. A summary of test results is given in Table 2. N63.2, the number of cycles to 63.2% failures [4], is used to express the characteristic life in this study.

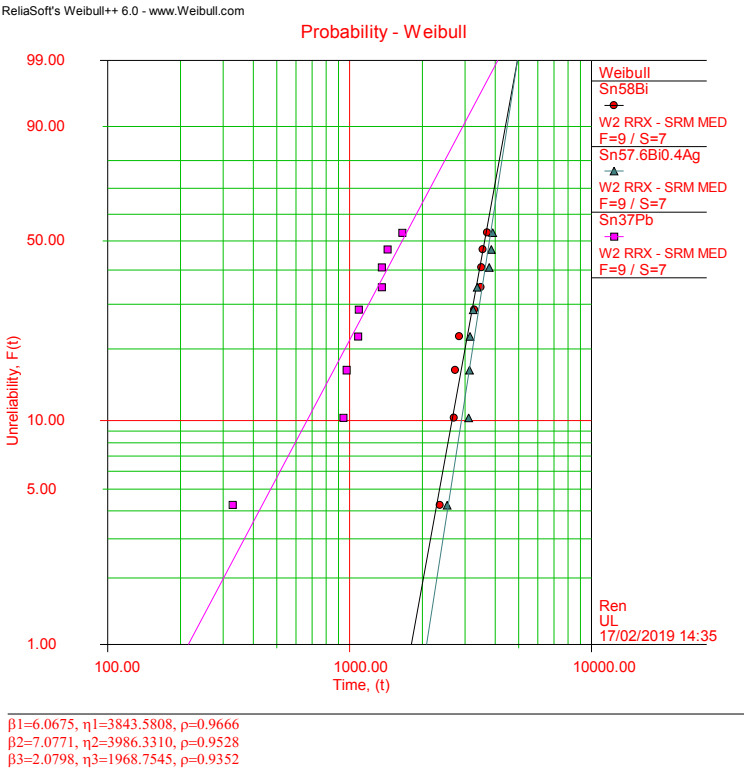


Figure 10. Weibull logarithm plot of solder joint lifetime for 1206 chip resistors.

Table 2. Result of board level solder joint reliability test

Solder	Characteristic lifetime η	Shape parameter β
Sn37Pb	1969	2.08
Sn58Bi	3844	6.07
Sn57.6Bi0.4Ag	3986	7.08

Both Sn58Bi and Sn57.6Bi0.4Ag solders show approximately doubled characteristic lifetime compared with conventional Sn37Pb solder. Upon micro-alloying Ag, lifetime of Sn58Bi is marginally increased. Their lifetime can be ranked as follows: Sn57.6Bi0.4Ag > Sn58Bi > Sn37Pb. Compared with Sn37Pb, Sn58Bi and Sn57.6Bi0.4Ag show much higher shape parameters, indicating solder joints failed within a relatively short time span.

4. Discussion

This phenomenon of microstructure refinement is commonly observed in micro-alloyed low temperature solder alloys [22–28, 38]. By micro-alloying Ag, the microstructure of Sn58Bi alloy becomes more refined whilst Ag₃Sn intermetallic compounds form, and these intermetallics enhance strength through a precipitation hardening mechanism which in turn deteriorates ductility due to their inherent brittleness.

The simultaneous combination of these two mechanisms: microstructure refinement and precipitation hardening improves the mechanical properties of Sn57.6Bi0.4Ag, and this manifests itself in an enhanced reliability performance. In addition, it is postulated that during thermal cycling Ag₃Sn intermetallic compounds are located at the Sn-Bi phase boundaries and they suppress the solder microstructure from coarsening through a grain boundary pinning effect, therefore extending the time to failure for these alloys.

5. Conclusions

By adding small amount of Ag (0.4 wt.%) into Sn58Bi solder alloy, the following can be concluded:

1. Mechanical properties, including tensile strength, yield strength, and Young's modulus are improved due to a combination of microstructural refinement and precipitation hardening.
2. Ductility is deteriorated due to the formation of brittle Ag₃Sn IMCs.
3. Board level reliability of solder joints is enhanced during ATC testing. Ag₃Sn IMCs are assumed to be located at the Sn-Bi phase boundaries and this leads to a suppression of coarsening in the solder microstructure.

Author Contributions: conceptualization, G.R. and M.C.; methodology, G.R.; validation, G.R. and M.C.; formal analysis, G.R.; investigation, G.R.; resources, G.R.; data curation, G.R.; writing—original draft preparation, G.R.; writing—review and editing, G.R. and M.C.; visualization, G.R.; supervision, M.C.; project administration, M.C.; funding acquisition, G.R. and M.C.

Funding: This work has been funded by the Irish Research Council in partnership with Henkel Ltd. under the Enterprise Partnership Scheme grant number EPSG/2014/48.

Conflicts of Interest: The authors declare no conflict of interest. The funders had no role in the design of the study; in the collection, analyses, or interpretation of data; in the writing of the manuscript, or in the decision to publish the results.

References

- [1] (21/01/2019). *Compliance FAQs: RoHS*. Available: <https://www.nist.gov/standardsgov/compliance-faqs-rohs>
- [2] H. R. Kotadia, P. D. Howes, and S. H. Mannan, "A review: On the development of low melting temperature Pb-free solders," *Microelectronics Reliability*, vol. 54, pp. 1253-1273, Jun-Jul 2014.
- [3] G. Henshall, R. Healey, R. S. Pandher, K. Sweatman, K. Howell, R. Coyle, *et al.*, "iNEMI Pb-free alloy alternatives project report: state of the industry," in *Proceedings SMTA International*, 2008.
- [4] D. Shangguan, *Lead-free solder interconnect reliability*: ASM international, 2005.
- [5] H. Ma and J. C. Suhling, "A review of mechanical properties of lead-free solders for electronic packaging," *Journal of Materials Science*, vol. 44, pp. 1141-1158, Mar 2009.
- [6] E. Bradley, C. A. Handwerker, J. Bath, R. D. Parker, and R. W. Gedney, *Lead-free electronics: iNEMI projects lead to successful manufacturing*: John Wiley & Sons, 2007.
- [7] K. Sukanuma, "Advances in lead-free electronics soldering," *Current Opinion in Solid State & Materials Science*, vol. 5, pp. 55-64, Jan 2001.
- [8] Y. Tang, G. Y. Li, and Y. C. Pan, "Influence of TiO₂ nanoparticles on IMC growth in Sn-3.0Ag-0.5Cu-xTiO(2) solder joints in reflow process," *Journal of Alloys and Compounds*, vol. 554, pp. 195-203, Mar 25 2013.
- [9] M. N. Collins, J. Punch, and R. Coyle, "Surface finish effect on reliability of SAC 305 soldered chip resistors," *Soldering & Surface Mount Technology*, vol. 24, pp. 240-248, 2012.
- [10] M. N. Collins, J. Punch, R. Coyle, M. Reid, R. Popowich, P. Read, *et al.*, "Thermal fatigue and failure analysis of SnAgCu solder alloys with minor Pb additions," *Components, Packaging and Manufacturing Technology, IEEE Transactions on*, vol. 1, pp. 1594-1600, 2011.
- [11] H. Fu, R. Aspandiar, J. Chen, S. F. Cheng, Q. Chen, R. Coyle, *et al.*, "Inemi Project on Process Development of Bisn-Based Low Temperature Solder Pastes - Part Ii: Characterization of Mixed Alloy Bga Solder Joints," *2018 Pan Pacific Microelectronics Symposium (Pan Pacific)*, 2018.
- [12] G. J. Jackson, I. J. Wilding, R. Boyle, M. N. Collins, E. Dalton, J. Punch, *et al.*, "SnZn Solder Alternative For Low-Cost Pb-Free Surface Mount Assemblies," in *SMTA International*, 2012.
- [13] G. Ren, I. J. Wilding, and M. N. Collins, "Alloying influences on low melt temperature SnZn and SnBi solder alloys for electronic interconnections," *Journal of Alloys and Compounds*, vol. 665, pp. 251-260, Apr 25 2016.
- [14] M. N. Collins, G. J. Jackson, E. Dalton, H. Steen, P. Liu, M. Holloway, *et al.*, "Accelerated Temperature Cycling and Microstructural Analysis of SnZn Solder In Surface Mount Assemblies," in *ICSR (Soldering and Reliability)*, 2012.
- [15] H. Lee, K. S. Choi, Y. S. Eom, H. C. Bae, and J. H. Lee, "Sn58Bi Solder Interconnection for Low-Temperature Flex-on-Flex Bonding," *Etri Journal*, vol. 38, pp. 1163-1171, Dec 2016.
- [16] S. Zhang and K. W. Paik, "A Study on the Failure Mechanism and Enhanced Reliability of Sn58Bi Solder Anisotropic Conductive Film Joints in a Pressure Cooker Test Due to Polymer Viscoelastic Properties and Hydros swelling," *Ieee Transactions on Components Packaging and Manufacturing Technology*, vol. 6, pp. 216-223, Feb 2016.
- [17] Y. Goh, A. S. M. A. Haseeb, and M. F. M. Sabri, "Effects of hydroquinone and gelatin on the electrodeposition of Sn-Bi low temperature Pb-free solder," *Electrochimica Acta*, vol. 90, pp. 265-273, Feb 15 2013.
- [18] W. B. Zhu, Y. Ma, X. Z. Li, W. Zhou, and P. Wu, "Effects of Al₂O₃ nanoparticles on the microstructure and properties of Sn58Bi solder alloys," *Journal of Materials Science-Materials in Electronics*, vol. 29, pp. 7575-7585, May 2018.
- [19] Y. Ma, X. Z. Li, W. Zhou, L. Z. Yang, and P. Wu, "Reinforcement of graphene nanosheets on the microstructure and properties of Sn58Bi lead-free solder," *Materials & Design*, vol. 113, pp. 264-272, Jan 5 2017.
- [20] Y. S. Shin, Y. K. Ko, J. K. Kim, S. Yoo, and C. W. Lee, "SiC-NANOPARTICLE DISPERSED COMPOSITE SOLDER BUMPS FABRICATED BY ELECTROPLATING," *Surface Review and Letters*, vol. 17, pp. 201-205, Apr 2010.
- [21] Y. Zuo, L. M. Ma, S. H. Liu, Y. T. Shu, and F. Guo, "WHISKER MITIGATION FOR Sn-BASED Pb-FREE SOLDER BY POSS ADDITION," *Acta Metallurgica Sinica*, vol. 51, pp. 685-692, Jun 11 2015.
- [22] K. Kanlayasiri and T. Ariga, "Physical properties of Sn58Bi-xNi lead-free solder and its interfacial reaction with copper substrate," *Materials & Design*, vol. 86, pp. 371-378, Dec 5 2015.
- [23] S. Q. Zhou, O. Mokhtari, M. G. Rafique, V. C. Shunmugasamy, B. Mansoor, and H. Nishikawa, "Improvement in the mechanical properties of eutectic Sn58Bi alloy by 0.5 and 1 wt% Zn addition before and after thermal aging," *Journal of Alloys and Compounds*, vol. 765, pp. 1243-1252, Oct 15 2018.

- [24] S. Q. Zhou, X. D. Liu, O. Mokhtari, and H. Nishikawa, "The evaluation of mechanical properties of Sn58BiXTi solder by tensile test," *2017 18th International Conference on Electronic Packaging Technology (Icept)*, pp. 703-707, 2017.
- [25] S. Sakuyama, T. Akamatsu, K. Uenishi, and T. Sato, "Effects of a third element on microstructure and mechanical properties of eutectic Sn-Bi solder," *Transactions of The Japan Institute of Electronics Packaging*, vol. 2, pp. 98-103, 2009.
- [26] W. X. Dong, Y. W. Shi, Z. D. Xia, Y. P. Lei, and F. Guo, "Effects of trace amounts of rare earth additions on microstructure and properties of Sn-Bi-based solder alloy," *Journal of Electronic Materials*, vol. 37, pp. 982-991, Jul 2008.
- [27] M. McCormack, H. S. Chen, G. W. Kammlott, and S. Jin, "Significantly improved mechanical properties of Bi-Sn solder alloys by Ag-doping," *Journal of Electronic Materials*, vol. 26, pp. 954-958, Aug 1997.
- [28] H. Y. Sun, Q. Q. Li, and Y. C. Chan, "A study of Ag additive methods by comparing mechanical properties between Sn57.6Bi0.4Ag and 0.4 wt% nano-Ag-doped Sn58Bi BGA solder joints," *Journal of Materials Science-Materials in Electronics*, vol. 25, pp. 4380-4390, Oct 2014.
- [29] K. Suganuma, T. Sakai, K. S. Kim, Y. Takagi, J. Sugimoto, and M. Ueshima, "Thermal and mechanical stability of soldering QFP with Sn-Bi-Ag lead-free alloy," *Ieee Transactions on Electronics Packaging Manufacturing*, vol. 25, pp. 257-261, Oct 2002.
- [30] W. Engelmaier, "Surface mount solder joint long-term reliability: Design, testing, prediction," *Soldering & Surface Mount Technology*, vol. 1, pp. 14-22, 1989.
- [31] R. Coyle, J. Osenbach, M. N. Collins, H. McCormick, P. Read, D. Fleming, *et al.*, "Phenomenological Study of the Effect of Microstructural Evolution on the Thermal Fatigue Resistance of Pb-Free Solder Joints," *Ieee Transactions on Components Packaging and Manufacturing Technology*, vol. 1, pp. 1583-1593, Oct 2011.
- [32] X. Huili, L. Tae-Kyu, and K. Choong-Un, "Fatigue properties of lead-free solder joints in electronic packaging assembly investigated by isothermal cyclic shear fatigue," in *Electronic Components and Technology Conference (ECTC), 2014 IEEE 64th*, 2014, pp. 133-138.
- [33] E. Dalton, G. Ren, J. Punch, and M. N. Collins, "Accelerated temperature cycling induced strain and failure behaviour for BGA assemblies of third generation high Ag content Pb-free solder alloys," *Materials & Design*, vol. 154, pp. 184-191, Sep 15 2018.
- [34] M. N. Collins, E. Dalton, and J. Punch, "Microstructural influences on thermomechanical fatigue behaviour of third generation high Ag content Pb-Free solder alloys," *Journal of Alloys and Compounds*, vol. 688, pp. 164-170, Dec 15 2016.
- [35] R. Coyle, M. Reid, C. Ryan, R. Popowich, P. Read, D. Fleming, *et al.*, "The Influence of the Pb-free Solder Alloy Composition and Processing Parameters on Thermal Fatigue Performance of a Ceramic Chip Resistor," *2009 Ieee 59th Electronic Components and Technology Conference, Vols 1-4*, pp. 423-430, 2009.
- [36] R. Coyle, J. Osenbach, P. Read, H. McCormick, D. Fleming, R. Popowich, *et al.*, "Dwell Time, Microstructural Dependencies, and the Interpretation of Thermal Fatigue Test Data of SnPb and Pb-free Solders," presented at the Dwell Time, Microstructural Dependencies, and the Interpretation of Thermal Fatigue Test Data of SnPb and Pb-free Solders, 2009.
- [37] R. Ghaffarian, "CCGA packages for space applications," *Microelectronics Reliability*, vol. 46, pp. 2006-2024, 12// 2006.
- [38] G. Ren and M. N. Collins, "The effects of antimony additions on microstructures, thermal and mechanical properties of Sn-8Zn-3Bi alloys," *Materials & Design*, vol. 119, pp. 133-140, 2017.
- [39] S. Liu, S. B. Xue, P. Xue, and D. X. Luo, "Present status of Sn-Zn lead-free solders bearing alloying elements," *Journal of Materials Science-Materials in Electronics*, vol. 26, pp. 4389-4411, Jul 2015.